# Original Research

# Decellularization of the human urethra for tissue engineering applications

**Marcela Kuniakova[1,2], Martin Klein[2,3], Paulina Galfiova[3], Maria Csobonyeiova[2,3], Claudia Feitscherova[2,3], Stefan Polak[3], Zuzana Varchulova Novakova[1,2], Katarina Topoliova[4], Branislav Trebaticky[2,4], Ivan Varga[2,3] (iD), Lubos Danisovic[1,2] (iD) and Stanislav Ziaran[2,4]**

[1]Institute of Medical Biology, Genetics and Clinical Genetics, Faculty of Medicine, Comenius University Bratislava 811 08, Slovakia; [2]National Institute of Rheumatic Diseases, Piestany 921 12, Slovakia; [3]Institute of Histology and Embryology, Faculty of Medicine, Comenius University Bratislava, Bratislava 811 08, Slovakia; [4]Department of Urology, Faculty of Medicine, Comenius University Bratislava, Bratislava 833 05, Slovakia
Corresponding author: Lubos Danisovic. Email: lubos.danisovic@fmed.uniba.sk

## Impact Statement

Despite the advances in biomedical research, the need for tissues for transplantation is still a significant medical problem. Recently, tissue engineering (TE) has the potential to solve this problem. Various scaffolding materials of natural and synthetic origin were fabricated, but many obstacles still need to be overcome in clinical practice. Hence, decellularized tissues with preserved architecture and biomechanical properties of native extracellular matrix (ECM) may have significant advantages in TE. This study confirms the feasibility of urethral decellularization based on combined (chemical, enzymatic, and mechanical) protocol. This protocol preserves the composition and ultrastructure of natural ECM while being non-toxic and DNA-free, which makes it an ideal scaffold for further experiments and TE applications.

## Abstract

Recently, several scaffolds have been introduced for urethral tissue engineering. However, acellular human urethral scaffold harvested from deceased donors may provide significant advantages compared to synthetic, composite, or other biological scaffolds. This study aims to develop the protocol for decellularization of the human urethra that preserves substantial extracellular matrix (ECM) components, which are essential for subsequent recellularization mimicking the natural environment of the native ECM. A total of 12 human urethras were harvested from deceased donors. An equal part of every harvested urethra was used as a control sample for analyses. The protocol design was based on the enzyme-detergent-enzyme method. Trypsin and Triton X-100 were used to remove cells, followed by DNase treatment to remove DNA residues. Subsequently, the specimens were continually rinsed in deionized water for seven days. The efficiency of decellularization was determined by histochemistry, immunohistochemical staining, scanning electron microscopy (SEM), and DNA quantification. Histological analysis confirmed cell removal and preservation of urethral structure after decellularization. The preservation of collagen IV and fibronectin was confirmed by histologic examination and immunohistochemical staining. SEM confirmed the maintenance of the ultra-structural architecture of ECM and fibers. DNA content in decellularized urethra was significantly lower compared to the native sample ($P < 0.001$), and so the criteria for decellularized tissue were met. Cytotoxicity analysis data showed that the matrix-conditioned medium did not contain soluble toxins and had no significant inhibitory effect on cell proliferation, providing evidence that the decellularized samples are not toxic. This study demonstrates the feasibility of the enzyme-detergent-enzyme–based decellularization protocol for removing cellular components and maintaining urethral ECM and its ultrastructure. Moreover, obtained results provide solid ground for recellularization and urethral tissue engineering, which will follow.

**Keywords:** Urethra, scaffold, decellularization, tissue engineering

## Introduction

The urethra, as the part of the human genitourinary tract, can be affected by numerous pathological conditions which negatively affect the quality of life and, in some cases, may lead to permanent organ impairment or even death. Impairment of the urethra often leads to scarring, which manifests as urethral stricture. Scar tissue has inferior biological and biomechanical features, but most importantly, it leads to a reduction of the urethral lumen (urethral stricture), with the subsequent formation of lower urinary tract obstruction (LUTS).[1]

The most crucial drawback of urethral strictures treatment (e.g. urethral dilation, direct vision internal urethrotomy – DVIU) is the relatively high risk of recurrence with patency rates between 8 and 77% for DVIU.[2,3] Length of stricture is the main predictive factor for stricture recurrence,[4] longer (more than 2 cm) strictures should be treated by open multi-staged urethroplasty with the use of lingual or buccal graft of skin flap to overcome the lack of functional tissue.[5] However, despite a relatively high recurrence-free and patency rate of 90.5%,[6] buccal or lingual graft harvesting is not complication free, especially in longer strictures.[7,8]

The development of tissue engineering (TE) has the potential to overcome these drawbacks. Functional, biocompatible scaffolds mimicking native ECM are cornerstones of TE.[9] They are prepared from various natural and synthetic polymers and can be sponges, fibers, and hydrogels.[10,11] These materials must meet several criteria – they must be sterile, non-toxic, biodegradable, and biocompatible.[9] Surface structure, porosity, and biomechanical properties of applied materials are also fundamental that influence their final application. Thanks to these properties, scaffolds have a mechanical function and can influence the adhesion of cells, their migration, proliferation, and differentiation to desirable phenotypes.[11] However, many obstacles (e.g. a complex protocol of their fabrication and modification, inferior biomechanical properties, etc.) still limit their application in clinical practice. Hence, decellularized tissues with preserved architecture and biomechanical properties of native ECM may have significant advantages in the context of urethral TE.[12,13] Besides being the body's material (autologous tissue), decellularized ECMs are very easy to obtain using simple, feasible, and effective processes resulting in the production of scaffolds containing collagen, elastin, glycosaminoglycans, and various bioactive molecules with the ability to provide an attractive microenvironment for cells.[14]

We developed a novel decellularization protocol for human urethras from deceased donors in this study. We evaluated the efficacy, feasibility, and biological safety of prepared acellular matrices *in vitro*, which can serve as an ideal scaffold for urethral TE.

## Materials and methods

### Human donor urethra harvesting

Harvesting of the human urethra was performed according to current regulations and after the permit from Institution for health-care providers' surveillance authority (no. 23/2022). Male urethras ($n = 12$) were harvested under antiseptic conditions from deceased adult donors aged 40–93 years after 24–72 h postmortem, after inserting a sterile permanent catheter as a guide wire. The skin was incised on the ventral side of the penis from the subcoronal area distally to the radix penis. Urethras were surgically dissected with corpus spongiosum with an average length of 7 cm ± 0.4 cm. After excision, the samples were placed in a sterile collection solution comprised of 500 mg Edicin (Sandoz, Switzerland), $2 \times 10^6$ U Penicillin (Biotika, Slovakia), 200 mg clotrimazole (Ratiopharm, Germany), 240 mg gentamycin (Sandoz, Switzerland) per liter of saline, and immediately transferred to the laboratory and left at 4°C for 3 h.

**Table 1.** Summary of decellularization method.

| Solution | Temperature, time |
|---|---|
| Collection solution | 4°C, 3 h |
| $dH_2O$ + ATB | 4°C, 24 h |
| 0.25% Trypsin-EDTA | 4°C, 24 h |
| $dH_2O$ | 4°C, $2 \times 10$ min |
| TRITON™ X-100 1:100 in $dH_2O$ | 4°C, 24 h |
| DNase I 200 µg/mL | 37°C, 3 h |
| $dH_2O$ | 4°C, seven days |

### Decellularization protocol

After 3 h in the collection solution, the samples were transferred to a new container with sterile deionized water ($dH_2O$) with antibiotic antimycotic solution (Merck, Germany) and washed on a shaker for 24 h at 4°C to wash out erythrocytes. Subsequently, the samples were transferred to a new container with 0.25% Trypsin-EDTA (Merck, Germany) solution and incubated with agitation on an orbital shaker at 4°C for 24 h. After washing in $dH_2O$ for $2 \times 10$ min, the samples were placed in a new container with TRITON™ X-100 (Merck, Germany) diluted 1:100 in $dH_2O$ and washed for 24 h at 4°C with agitation on an orbital shaker. In the next step, samples were incubated for 3 h at 37°C in DNase I (200 µg/mL; Roche, Switzerland). Samples were then washed in $dH_2O$ with gentle agitation for seven days at 4°C. Water was changed daily. In Table 1, the summary of procedures is presented. At the end of the decellularization process, several microbiological tests were routinely performed to guarantee tissue sterility in the protocol.

### Light microscopy and immunohistochemistry

For light microscopy, the native controls and decellularized tissue samples of human male penile urethras collected during the autopsy were processed by the routine formalin-fixed, paraffin-embedded technique. Specimens were fixed in 10% neutral buffered formalin (CentralChem, Slovakia) for 24 h at room temperature, dehydrated in alcohol series of increasing concentrations up to 100%, cleared with xylene (Merck, Germany), immersed in paraffin (Merck, Germany), and finally embedded in paraffin tissue blocks. The blocks were then cut into 5 µm thick sections by a rotary microtome, transferred onto glass slides, deparaffinized using xylene, and rehydrated in alcohol series of decreasing concentrations to 50%. Finally, the slides were stained with hematoxylin and eosin (HE), green trichrome, and orcein (all by Merck, Germany) to visualize cell nuclei, collagen fibers, and elastic fibers, respectively.

For immunohistochemistry, antibodies against collagen IV and fibronectin (Merck, Germany) to visualize different components of the extracellular matrix (ECM). The pretreatment processes of deparaffinization, rehydration, and epitope unmasking were carried out automatically using PT Link (Agilent Technologies, Santa Clara, CA, USA). The specimens were treated with a Peroxidase-Blocking Reagent of the EnVision FLEX Detection system (Agilent Technologies) for 5 min to block endogenous peroxidase activity. The primary antibodies were applied

according to the manufacturer's protocols. For visualization, Diaminobenzidine (DAB) + Chromogen of the EnVision FLEX Detection system (Agilent Technologies) was used. For better orientation within the native control specimens, cell nuclei were counterstained with Mayer's hematoxylin (Merck, Germany). The slides were examined by an LEICA DM2500 microscope, and representative fields of view were captured on the LEICA DFC290HD digital camera.

## Scanning electron microscopy

For scanning electron microscopy (SEM), the native controls and decellularized tissue samples of human male penile urethras (the maximum size of $600\,mm^3$) collected during an autopsy were fixed in 3% buffered glutaraldehyde (Merck, Germany) for 4h at room temperature. Afterward, the samples were rinsed three times in sodium phosphate buffer (pH = 7.3; Merck, Germany) and postfixed in osmium tetroxide solution (Merck, Germany) at 4°C. Next, the samples were gently dehydrated using alcohol series of increasing concentrations up to 100% and dried at the critical point of $CO_2$ using Critical Point Dryer BAL-TEC CPD 030. Then, the specimens were mounted on aluminum specimen stubs using carbon adhesive tapes. The non-conductive specimens were sputter-coated with a 15-nm thick gold/palladium layer in the LEICA EM ACE200 sputter coater and observed by the ZEISS EVO LS 15 scanning electron microscope.

## Analysis of DNA content

The isolation, quantification, and quality of DNA in the decellularized urethra were performed using the protocol of GeneJET Genomic DNA Purification Kit (Thermo Fisher Scientific, Waltham, MA, USA) and agarose gel electrophoresis. Native urethras of the same origin served as a positive control ($n = 12$). In brief, native and decellularized urethral tissue was cut into small pieces and dried to constant weight at 37°C. A precisely weighed sample was then resuspended in Digestion Solution with Proteinase K (Thermo Fisher Scientific) and incubated at 56°C overnight. After incubation, RNase solution (Thermo Fisher Scientific) was added and set for 10min at room temperature. Lysis solution was then added and vortexed until a homogeneous suspension was obtained. After vortexing, a 50% ethanol solution (CentralChem) was added, and the lysate was transferred to a GeneJET Genomic DNA Purification Column (Thermo Fisher Scientific) and centrifugated. After two washing steps, the Purification Column was transferred to a sterile microcentrifuge tube, and an Elution Buffer was added to elute genomic DNA. The concentration of extracted DNA was measured spectrophotometrically using the NanoDrop Spectrophotometer (Thermo Fisher Scientific), and the final amount of DNA (ng/DNA per mg/tissue dry weight) was calculated.

For qualitative fragment length analysis, 10 μL of total DNA was separated in 1.5% agarose gel (40min, 120V). After the run, the gel was documented by Azure C300 Imaging System (Azure Biosystems, Dublin, CA, USA).

## Cytotoxicity assay – growth inhibition assay

To determine whether the decellularized sample contains any soluble toxins, we used the 3-(4,5-dimethyl-2-thiazolyl)-2,5-diphenyl-2H-tetrazolium bromide (MTT) assay to evaluate the cytotoxic effect of the matrix-conditioned medium on cells. Cell proliferation served as an indicator of the material biocompatibility, which was detected by MTT. First, $5\,cm^2$ of decellularized tissue was cut into small pieces, added to 50 mL of Dulbecco's Modified Eagle Medium (DMEM) (Merck, Germany), and washed on a shaker for 24h at 37°C. After 24h, the medium was filtered through a 0.2-μm filter, and 10% fetal bovine serum (FBS, Merck, Germany) was added. Unconditioned DMEM supplemented by 10% FBS was used as a negative control. Adipose tissue–derived stem cells (ATSCs) were seeded in a 96-well plate at a concentration of $7 \times 10^3$ cells per well in replicates of six. The plates were incubated at 37°C in a humidified atmosphere of 5% $CO_2$ in the air for seven days. One plate was removed on days 1, 3, 5, and 7 to assess cell viability with the MTT assay. 20 μL of CellTiter 96 AQueosus One Solution Cell Proliferation Assay (Promega, Madison, WI, USA) was pipetted into each well containing 100 μL of culture medium. The plate was incubated for 3h at 37°C in a humidified, 5% $CO_2$ atmosphere. Absorbance was recorded at 490 nm using a 96-well plate reader BioTek EL 800 (BioTek, Winooski, VT, USA). Test samples are assigned to the control samples where the proliferation reaches a value of 100%. Obtained data were analyzed and processed into graphs.

## Statistical analysis

DNA content analysis results are reported as mean ± standard deviation (SD), with a statistical significance of $P < 0.001$. To compare and analyze the concentration of DNA isolated from dry tissue (ng/DNA per mg/tissue dry weight) from native urethra samples with decellularized urethra samples with respect to each other, a Student's *t*-test was employed. The proliferation rate is reported as mean ± SD, and absorbance values were expressed as mean ± SD. One-way analysis of variance (ANOVA) followed by the Bonferroni and Holm posthoc tests for multiple comparisons were used when appropriate. $P < 0.01$ and $P < 0.05$ were considered statistically significant.

# Results

## Decellularization of urethra

Human urethral samples were decellularized by the enzyme-detergent-enzyme method using Trypsin, Triton X-100, and DNase, and subsequently characterized to verify decellularization success by histology, SEM, and analysis of remaining DNA. Safety was confirmed by sterility and cytotoxicity testing. The effectiveness of the decellularization process was first assessed by macroscopic appearance. Native urethra samples display a pinkish appearance (Figure 1(a)). The urethral tissue, after decellularization, showed a change in color to milky white and slightly translucent (Figure 1(b)) which suggests the gradual removal of cells. A milder color change was rarely observed in the middle part of the sample; however, histological analyzes did not confirm a reduced degree of decellularization in that part. Cultures from samples at the final step in the decellularization protocol were negative for aerobic and anaerobic bacteria, fungi, and yeasts.
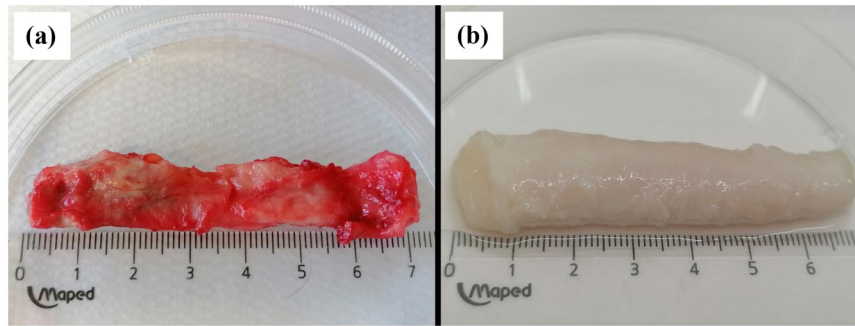
**Figure 1.** Macroscopic appearance of the urethra before (a) and after (b) decellularization.

## Preservation of histological morphology

HE-stained native controls (Figure 2(a)) clearly showed the typical cellular composition of the mucosa: stratified columnar epithelium, different types of fixed and wandering cells of the loose collagenous connective tissue of the lamina propria, and blood vessels. HE-stained decellularized urethras (Figure 2(b)) had no visible cell nuclei within the mucosa nor in the muscle layer (no purple staining visible). The only observable structures were different eosinophilic (pink) components of the ECM. Figure 2(c) and (d) demonstrates that the decellularization process preserved elastic fibers, and there were no evident differences in their composition and quantity. Brown-red fibers were clearly visible in all the layers of the urethra in both the native controls and decellularized specimens. Comparing native controls (Figure 2(e)) with decellularized specimens (Figure 2(f)), there were no observable differences in the quantitative or qualitative characteristics of type I collagen fibers (green color) that could be detected at the level of light microscopy. Trichrome-stained native controls (Figure 2(e)) also showed multiple cell nuclei within the mucosa's epithelial lining and connective tissue. Red blood cells were also visible inside the lumen of blood vessels.

After immunohistochemical (IHC) visualization of collagen IV in native tissues (Figure 2(g)), the most robust positivity was observed within the basement membranes of blood vessels. Anticollagen IV positivity in decellularized specimens was well preserved (Figure 2(h)) without any apparent changes. IHC demonstration of fibronectin in native specimens (Figure 2(i)) showed that this structural glycoprotein of the ECM is widely distributed within the ground substance. After decellularization (Figure 2(j)), fibronectin appeared to be minimally affected by the process in terms of its quantity and distribution.

## SEM

SEM analysis revealed a similar ECM architecture between the native urethra and decellularized samples. Cell population on the luminal urethral surface and structure of the ECM components in lamina propria were evaluated in both sample groups (native and decellularized). Native urethra sample surface displayed an epithelial lining, particularly with columnar epithelial cells of stratified epithelium attached to the basal lamina (Figure 3(a)). Cross-section by the wall of the urethra, or even more accidentally exposed surfaces of deep layers showed a content of the underlying lamina propria. Collagen fibers were ordinarily fashioned in wave-like bundles running in more directions, and loose collagenous connective tissue cells were not identified. The surface of decellularized samples contained no epithelial cells and reflected a smooth surface of the basal lamina (Figure 3(b)). Areas of slightly weakened basal lamina were rarely present but considered artifacts. Collagen fibers of ECM in decellularized samples manifested a similar pattern of ultrastructure as in native samples. No elevated disarrangement or tissue damage in electroconvulsive therapy (ECT) was noticed. Quantification was not performed due to unequal sample surfaces. We may sum up that no significant changes in ECM ultrastructure were found when comparing the structure of the native urethra sample and decellularized samples.

## DNA quantification and qualitative fragment analysis

In addition to the absence of visible nuclei after HE staining in decellularized tissue, the basic condition for successful decellularization is the fulfillment of two other criteria: the amount of DNA must not exceed 50 ng per mg of dry tissue weight and the remaining DNA fragments must not be larger than 200 bp. The DNA content in native urethras was $528.1 \pm 191.7$ ng/mg tissue, and residual DNA content in decellularized samples was $26.9 \pm 12.4$ ng/mg tissue (Figure 4(a)). Statistical analysis confirmed a significant difference in the amount of residual DNA ($P < 0.001$; $n = 12$). Qualitative analysis of DNA fragments by gel electrophoresis showed intact DNA bands in native urethral samples larger than 3000 bp (Figure 4(b)). In the decellularized samples, the analysis confirmed significant removal of DNA.

## Cytotoxicity

The results of the viability assessed by the MTT test (Figure 5) evaluated on the first, third, fifth, and seventh day show that ATSC cells can grow in both control and matrix-conditioned medium. Test samples are assigned to the control samples where the viability reaches 100%. Data showed that the matrix-conditioned medium did not contain soluble toxins and did not have any significant inhibitory effect on cell viability, providing evidence that the decellularized samples are not toxic. Viability reached an average value of 108% on the first day, followed by 103% on the third day, 103% on the fifth day, and
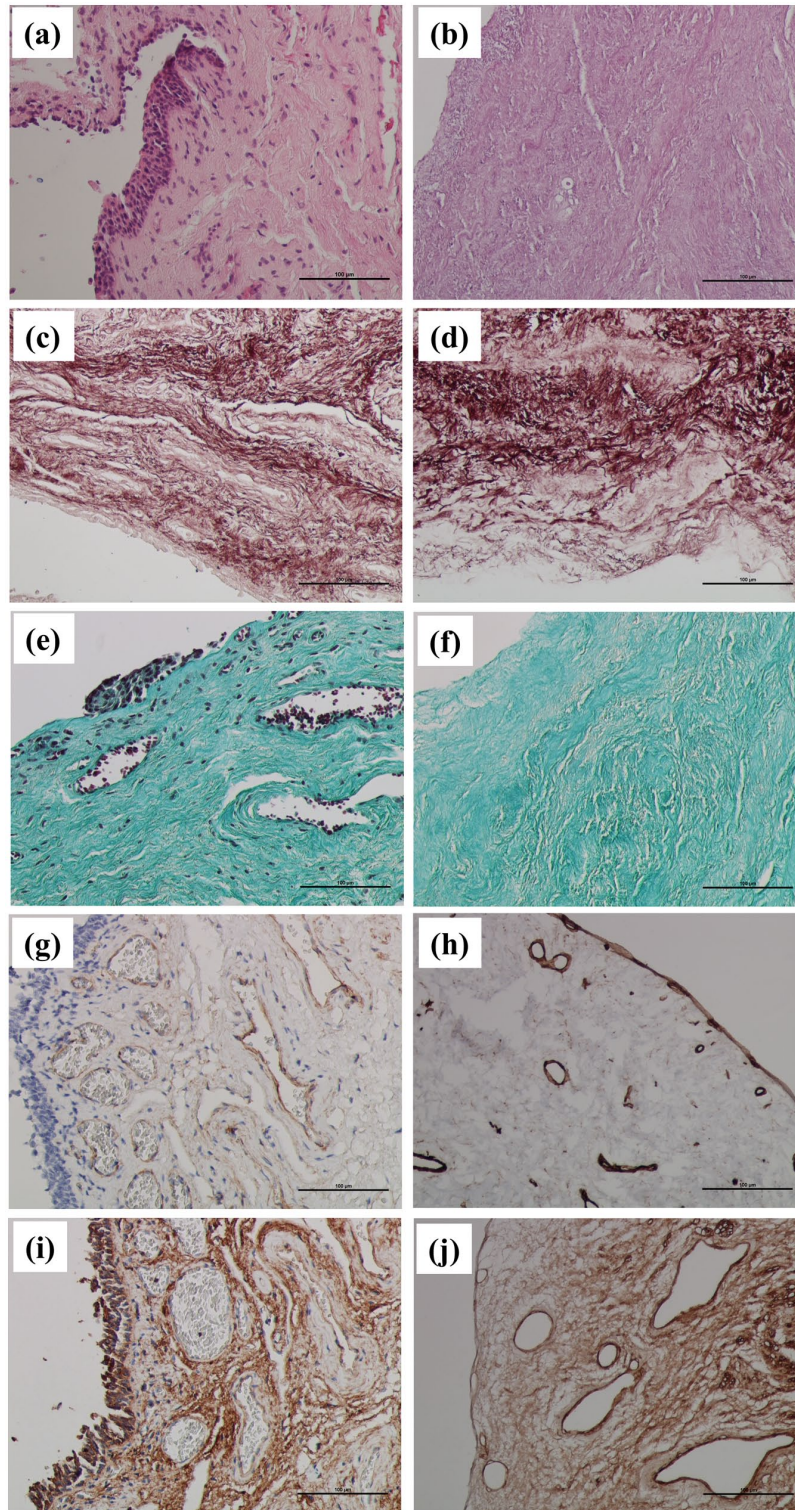
**Figure 2.** (a) Native control of human male penile urethra. HE staining. Original magnification 200×. Normal mucosa with stratified columnar epithelium and connective tissue of lamina propria. Clearly visible purple basophilic cell nuclei (arrows) and pink components of the ECM; (b) Decellularized human male penile urethra. HE staining. Original magnification 200×. No purple basophilic cell nuclei are visible after decellularization, only pink-stained eosinophilic components of the ECM; (c) native control of human male penile urethra. Orcein staining. Original magnification 200×. Red-brown stained elastic fibers are well visible within the connective tissue of lamina propria (arrows); (d) decellularized human male penile urethra. Orcein staining. Original magnification 200×. Decellularization preserved the red-brown elastic fibers of the connective tissue (arrows); (e) native control of human male penile urethra. Green trichrome staining. Original magnification 200×. Green collagen fibers (arrows) and brown-black cell nuclei (arrows) are visible within the mucosa; (f) decellularized human male penile urethra. Green trichrome staining. Original magnification 200×. Decellularization preserved green collagen fibers (arrows) but completely eliminated cell nuclei; (g) native control of human male penile urethra. IHC. Anticollagen IV. Original magnification 200×. Collagen IV (brown) is located mainly within the basement membranes of blood vessels. Counterstaining with Mayer's hematoxylin visualized blue cell nuclei in the epithelium and connective tissue (arrows); (h) decellularized human male penile urethra. IHC. Anticollagen IV. Original magnification 200×. Decellularization preserved collagen IV (brown) within the basement membranes but completely eliminated cell nuclei; (i) native control of human male penile urethra. IHC. Antifibronectin. Original magnification 200×. Structural glycoprotein fibronectin (brown) is found abundantly within the ground substance of the connective tissue ECM. Counterstained cell nuclei of the epithelial lining and lamina propria are stained blue (arrows); (j) decellularized human male penile urethra. IHC. Antifibronectin. Original magnification 200×. After decellularization, fibronectin is well preserved (brown), with no visible cell nuclei.
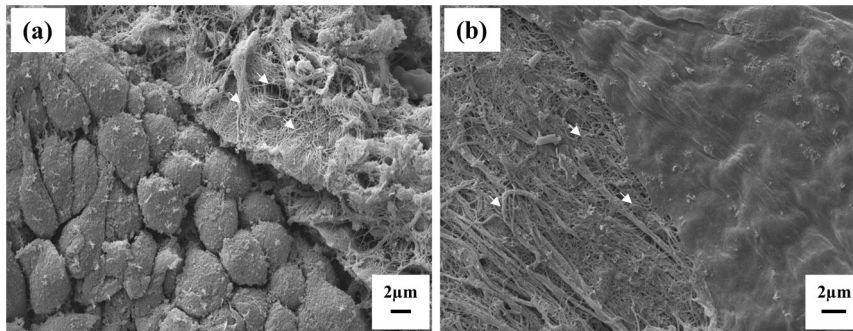
**Figure 3.** (a) Surface of male urethra mucosa in reference autopsy sample. Evidence of tightly packed epithelial cells with polygonal surface view shape which are oriented to the urethral lumen. Epithelial cells form a stratified columnar mucosa lining (down left), but only superficial columnar cells are evident on the top. The basal lamina of epithelial cells is not visible in a surface view. Accidentally exposed surface of the lamina propria content (upper right) revealed bundles of collagen fibers (arrows) are in loose collagenous connective tissue in the compact pattern (slight contamination by artificial crystals of phosphate buffer). Original magnification 2000×. (b) Surface of male urethra mucosa in sample processed by decellularization. The surface represents only the basal lamina with no epithelial cells. The basal lamina has a smooth surface, with delicate rare openings (upper right). The basal lamina is attached to underlying loose collagenous connective tissue. Collagen fibers form bundles (arrows) or run in a free pattern. Original magnification 3000×.
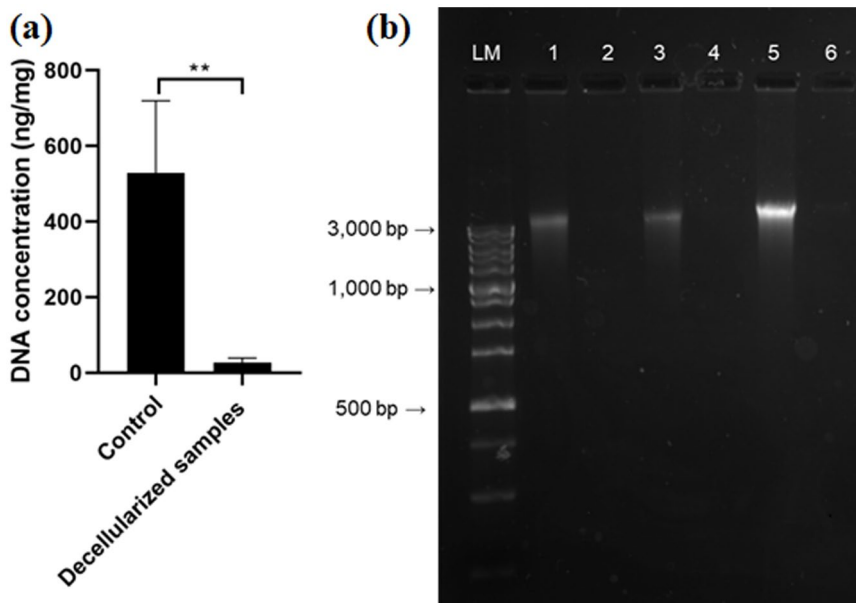


**Figure 4.** (a) Quantification of DNA in native and decellularized sample (ng/DNA per mg/tissue dry weight). Results as mean ± SD, $n = 12$, **$P \leqslant 0.001$, $t$-test; (b) qualitative fragment length analysis of genomic DNA in 1.5% agarose gel.
LM: length ladder; 1, 3, and 5: native urethra samples; 2, 4, and 6: corresponding decellularized urethra samples.

99% on the seventh day of cultivation. Statistical significance was not confirmed.

## Discussion

Because the number of organ donors cannot meet the needs of patients waiting for a transplant, research in the field of TE and regenerative medicine seeks to provide alternative treatment strategies. Various scaffolds of natural (e.g. collagen, elastin, cellulose, etc.) and synthetic origin (e.g. PLA, PLGA, PHB, etc.) for urethral TE were extensively studied in preclinical and clinical trials.[15–18] Besides that, one of the most promising tissue and organ regeneration methods is decellularization, in which the ECM is isolated from the native tissues to create a natural structure. The ECM – which ideally retains its complex composition, vascular networks, tissue-specific architecture, and biochemical and biomechanical

properties – can then be repopulated with cells to form a functional tissue or organ.[19]

In the past decades, there has been an increase in publications dealing with the decellularization of different tissues or whole organs.[20–22] Studies with tissue-engineered urethral substitutes also grew in numbers. Regarding scaffolds, the cornerstones of TE, a plethora of materials were used in preclinical and clinical settings, including porcine small intestine submucosa, cadaveric bladder acellular matrix graft, and human acellular dermal matrix, to name just a few.[19] In preclinical studies, decellularized animal urethras from dogs, porcine, and rabbits were performed to evaluate their potential for application in urethral regeneration.[23–25] Several scientific groups have been trying to decellularize various parts of the urogenital tract, including the foreskin,[26] urethra,[27,28] ureter,[29] and bladder[30,31] up to the complete human phallus,[32] to solve complex urogenital and penile defects.
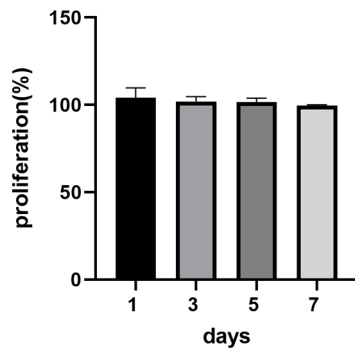
**Figure 5.** Proliferation assessed by MTT test results. Test sample proliferation values on specific days are assigned to control samples where proliferation reaches a value of 100%. Data are presented as the mean ± SD. No significant decrease in the cell proliferation rate was detected when co-cultured with the matrix-conditioned medium.

However, no decellularized human urethras we used in a clinical setting so far. This may be surprising since autologous biological scaffolds can preserve natural ECM compounds that mimic the original microenvironment. This may improve natural tissue regeneration compared to synthetic or composite scaffolds.[33]

Decellularization can be achieved using chemical, enzymatic, physical, or combined methods. Different protocols have distinct effects on the extent of cell removal and ECM composition and structure.[34] This decellularization protocol is newly developed and combines the use of a hypotonic solution, enzymes, and detergent. The urethral tissue surrounded by the corpus spongiosum was decellularized in a native tubular form. Deionized water was used for osmotic lysis of the cells, enzymatic treatment with trypsin to disrupt cell–cell adhesion and cell–ECM adhesion, low-concentration ionic detergent Triton X-100 to remove cellular components and tissue debris, and in the final step DNase I to remove DNA residues. The decellularized tissue was washed in deionized water for seven days to remove any residual chemical or biological agents. All washing steps were performed on an orbital shaker with mechanical agitation to increase the protocol's effectiveness. A similar dynamic scheme of decellularization was introduced by Simões and co-workers on the porcine model.[27] Moreover, they combined mechanical agitation with perfusion force to promote a more efficient and homogeneous cellular removal from urethra tissue. In another study, Consolo and co-workers also showed that combining mechanical and chemical decellularization methods is more efficient in removing cellular content and maintaining the main tissue architecture and properties than chemical approaches alone.[35] Also, in this study, the histological analysis (histochemistry and SEM) of decellularized samples compared to the control samples confirmed excellent preservation of the amount and distribution of collagen fibers, elastin, and fibronectin, which are key components of the ECM. Since most adult cells have a deficient ability to synthesize elastin and remodel elastic matrix structures, the preservation of collagen and elastin represents a huge advantage of decellularized tissue over other substitutes (e.g. synthetic polymers). Well-preserved fibronectin, which is an adhesion molecule involved in the adhesion, growth, and migration of cells, as well as other

glycosaminoglycans, together with the three-dimensional (3D) architecture of collagen fibers, play an essential role in the ability of cells to migrate to the scaffold, settle there and multiply, which is the goal in tissue regeneration.[36]

Another prerequisite before the potential clinical application of tissue-engineered substitutes is an assessment of the potential cytotoxicity.[9] Even though sodium dodecyl sulfate (SDS) can offer adequate cellular component removal, utilization of SDS in the decellularization procedure may compromise the cytocompatibility of the scaffolding materials. It was reported that SDS remains in decellularized tissues may act as a cytotoxic agent.[37,38] Consecutive washing in phosphate-buffered saline (PBS) and distilled water results in a significant reduction in SDS concentration. Moreover, applying Triton X-100 also successfully lowers the SDS concentration in the materials, thus improving the cytocompatibility of the decellularized tissues.[39,40]

In this study, cytotoxicity testing did not show any inhibitory effect of the matrix-conditioned medium on cell viability compared to the control, indicating that the washing steps are sufficient. The analysis of residual DNA also confirmed the effectiveness of the decellularization protocol. After decellularization, there was a significant decrease in the amount of DNA present compared to the control below the limit set for tissue decellularization, which is 50 ng per mg of dry tissue weight.[27] This was also confirmed by the qualitative analysis of DNA fragments.

Overall, these data showed that this simple and feasible mechano-chemical method effectively removes the cellular component in the entire sample length and, at the same time, is gentle enough on the ECM of the native tissue. Although this protocol represents a solid ground, further analysis is required before introducing this methodology into routine practice, mainly focused on potential biosafety issues (e.g. immunogenicity, biocompatibility, etc.) and more precise preservation of morphological and biological properties of ECM, both *in vitro* and *in vivo*. Mentioned is the main prerequisite prior to ECM recellularization. Moreover, a wide range of biomechanical testing will follow.

## Conclusions

An ideal scaffold imitates the natural environment, represents mechanical support, preserves macro and micro architecture, integrity, and vasculature, and is recognized by cells that can adhere, differentiate, and mature in it. Cadaveric organ-specific matrices, after decellularization, can provide a suitable native microenvironment for cell homing and tissue regeneration. This study confirms the feasibility of urethral decellularization based on combined (chemical, enzymatic, and mechanical) protocol. This protocol preserves the composition and ultrastructure of natural ECM while being non-toxic and DNA-free, which makes it an ideal scaffold for further experiments and TE applications.

**AUTHORS' CONTRIBUTIONS**

Each author has met the EBM authorship requirements. MKu, IV, LD, and SZ conceptualized and designed the study; MKu, MKl, PG, MC, CF, SP, and ZVN performed experiments; KT, BT, and SZ were involved in sampling procedures; MKu, IV, LD, and SZ analyzed data and interpreted results of experiments;

**ORCID IDS**

Ivan Varga 🆔 https://orcid.org/0000-0002-0918-741X
Lubos Danisovic 🆔 https://orcid.org/0000-0002-5074-9621

**REFERENCES**

1. Davis NF, Quinlan MR, Bhatt NR, Browne C, MacCraith E, Manecksha R, Walsh MT, Thornhill JA, Mulvin D. Incidence, cost, complications and clinical outcomes of iatrogenic urethral catheterization injuries: a prospective multi-institutional study. *J Urol* 2016;**196**:1473–7

2. Al Taweel W, Seyam R. Visual internal urethrotomy for adult male urethral stricture has poor long-term results. *Adv Urol* 2015;**2015**: 656459

3. Redón-Gálvez L, Molina-Escudero R, Álvarez-Ardura M, Otaola-Arca H, Alarcón Parra RO, Páez-Borda Á. Factores predictivos de recidiva de estenosis uretral tras uretrotomía endoscópica. *Actas Urológicas Españolas* 2016;**40**:529–33

4. Steenkamp JW, Heyns CF, de Kock ML. Internal urethrotomy versus dilation as treatment for male urethral strictures: a prospective, randomized comparison. *J Urol* 1997;**157**:98–101

5. EAU. EAU guidelines. In: *Edn. presented at the EAU Annual Congress Milan 2021*, Arnhem, EAU, 2021

6. Mangera A, Patterson JM, Chapple CR. A systematic review of graft augmentation urethroplasty techniques for the treatment of anterior urethral strictures. *Eur Urol* 2011;**59**:797–814

7. Sinha RJ, Singh V, Sankhwar S, Dalela D. Donor site morbidity in oral mucosa graft urethroplasty: implications of tobacco consumption. *BMC Urol* 2009;**9**:15

8. Jang TL, Erickson B, Medendorp A, Gonzalez CM. Comparison of donor site intraoral morbidity after mucosal graft harvesting for urethral reconstruction. *Urology* 2005;**66**:716–20

9. Sahakyants T, Vacanti JP. Tissue engineering: from the bedside to the bench and back to the bedside. *Pediatr Surg Int* 2020;**36**:1123–33

10. Chen M, Jiang R, Deng N, Zhao X, Li X, Guo C. Natural polymer-based scaffolds for soft tissue repair. *Front Bioeng Biotechnol* 2022;**10**:954699

11. Jain P, Rauer SB, Möller M, Singh S. Mimicking the natural basement membrane for advanced tissue engineering. *Biomacromolecules* 2022;**23**: 3081–103

12. Zhu D, Jiang Z, Li N, Wang X, Ren L, Ye Y, Pan Y, Yang G. Insights into the use of genetically modified decellularized biomaterials for tissue engineering and regenerative medicine. *Adv Drug Deliv Rev* 2022;**188**: 114413

13. Hortensius RA, Harley BA. Naturally derived biomaterials for addressing inflammation in tissue regeneration. *Exp Biol Med (Maywood)* 2016; **241**:1015–24

14. Zhang X, Chen X, Hong H, Hu R, Liu J, Liu C. Decellularized extracellular matrix scaffolds: recent trends and emerging strategies in tissue engineering. *Bioact Mater* 2022;**10**:15–31

15. Gallo N, Natali ML, Curci C, Picerno A, Gallone A, Vulpi M, Vitarelli A, Ditonno P, Cascione M, Sallustio F, Rinaldi R, Sannino A, Salvatore L. Analysis of the physico-chemical, mechanical and biological properties of crosslinked type-i collagen from horse tendon: towards the development of ideal scaffolding material for urethral regeneration. *Materials* 2021;**14**:7648

16. Hu J, Ai B, Zhu S, Wang Z, Xia H, Jia W. Electrospun PLGA and PLGA/gelatin scaffolds for tubularized urethral replacement: studies in vitro and in vivo. *J Biomater Appl* 2022;**36**:956–64

17. Findrik Balogová A, Hudák R, Tóth T, Schnitzer M, Feranc J, Bakoš D, Živ ák J. Determination of geometrical and viscoelastic properties of PLA/PHB samples made by additive manufacturing for urethral substitution. *J Biotechnol* 2018;**284**:123–30

18. Zhu Z, Yang J, Ji X, Wang Z, Dai C, Li S, Li X, Xie Y, Zheng Y, Lin J, Zhou L. Clinical application of a double-modified sulfated bacterial cellulose scaffold material loaded with FGFR2-modified adipose-derived stem cells in urethral reconstruction. *Stem Cell Res Ther* 2022;**13**:463

19. Versteegden LRM, de Jonge PKJD, IntHout J, van Kuppevelt TH, Oosterwijk E, Feitz WFJ, de Vries RBM, Daamen WF. Tissue engineering of the urethra: a systematic review and meta-analysis of preclinical and clinical studies. *Eur Urol* 2017;**72**:594–606

20. Schleifenbaum S, Prietzel T, Aust G, Boldt A, Fritsch S, Keil I, Koch H, Möbius R, Scheidt HA, Wagner MF, Hammer N. Acellularization–induced changes in tensile properties are organ specific – an in-vitro mechanical and structural analysis of porcine soft tissues. *PLoS ONE* 2016;**11**:e0151223

21. Remlinger NT, Wearden PD, Gilbert TW. Procedure for decellularization of porcine heart by retrograde coronary perfusion. *Jove* 2012;**70**: e50059

22. Keshvari MA, Afshar A, Daneshi S, Khoradmehr A, Baghban M, Muhaddesi M, Behrouzi P, Miri MR, Azari H, Nabipour I, Shirazi R, Mahmudpour M, Tamadon A. Decellularization of kidney tissue: comparison of sodium lauryl ether sulfate and sodium dodecyl sulfate for allotransplantation in rat. *Cell Tissue Res* 2021;**386**:365–78

23. Shokeir A, Osman Y, El-Sherbiny M, Gabr M, Mohsen T, El-Baz M. Comparison of partial urethral replacement with acellular matrix versus spontaneous urethral regeneration in a canine model. *Eur Urol* 2003;**44**:603–9

24. Sievert KD, Wefer J, Bakircioglu ME, Nunes L, Dahiya R, Tanagho EA. Heterologous acellular matrix graft for reconstruction of the rabbit urethra: histological and functional evaluation. *J Urol* 2001;**165**:2096–102

25. Hu YF, Yang SX, Wang LL, Jin HM, Zhan BY. Reconstruction of rabbit urethra using urethral extracellular matrix. *Zhonghua Zheng Xing Wai Ke Za Zhi* 2009;**25**:54–7

26. Purpura V, Bondioli E, Cunningham EJ, De Luca G, Capirossi D, Nigrisoli E, Drozd T, Serody M, Aiello V, Melandri D. The development of a decellularized extracellular matrix–based biomaterial scaffold derived from human foreskin for the purpose of foreskin reconstruction in circumcised males. *J Tissue Eng* 2018;**9**:2041731418812613

27. Simões IN, Vale P, Soker S, Atala A, Keller D, Noiva R, Carvalho S, Peleteiro C, Cabral JMS, Eberli D, da Silva CL, Baptista PM. Acellular urethra bioscaffold: decellularization of whole urethras for tissue engineering applications. *Sci Rep* 2017;**7**:41934

28. Kajbafzadeh AM, Abbasioun R, Sabetkish S, Sabetkish N, Rahmani P, Tavakkolitabassi K, Arshadi H. Future prospects for human tissue engineered urethra transplantation: decellularization and recellularization-based urethra regeneration. *Ann Biomed Eng* 2017;**45**:1795–806

29. Koch H, Hammer N, Ossmann S, Schierle K, Sack U, Hofmann J, Wecks M, Boldt A. Tissue engineering of ureteral grafts: preparation of biocompatible crosslinked ureteral scaffolds of porcine origin. *Front Bioeng Biotechnol* 2015;**3**:89

30. Bolland F, Korossis S, Wilshaw SP, Ingham E, Fisher J, Kearney JN, Southgate J. Development and characterisation of a full-thickness acellular porcine bladder matrix for tissue engineering. *Biomaterials* 2007;**28**:1061–70

31. Rosario DJ, Reilly GC, Ali Salah E, Glover M, Bullock AJ, Macneil S. Decellularization and sterilization of porcine urinary bladder matrix for tissue engineering in the lower urinary tract. *Regen Med* 2008;**3**:145–56

32. Tan Y, Landford WN, Garza M, Suarez A, Zhou Z, Coon D. Complete human penile scaffold for composite tissue engineering: organ decellularization and characterization. *Sci Rep* 2019;**9**:16368

33. Sivaraman B, Bashur CA, Ramamurthi A. Advances in biomimetic regeneration of elastic matrix structures. *Drug Deliv Transl Res* 2012;**2**:323–50

34. Maghsoudlou P, Totonelli G, Loukogeorgakis SP, Eaton S, De Coppi P. A decellularization methodology for the production of a natural acellular intestinal matrix. *Jove* 2013;**80**:50658

35. Consolo F, Brizzola S, Tremolada G, Grieco V, Riva F, Acocella F, Fiore GB, Soncini M. A dynamic distention protocol for whole-organ bladder decellularization: histological and biomechanical characterization of the acellular matrix: whole bladder dynamic decellularization. *J Tissue Eng Regen Med* 2016;**10**:E101–12

36. Ribeiro-Filho LA, Sievert K-D. Acellular matrix in urethral reconstruction. *Adv Drug Deliv Rev* 2015;**82–83**:38–46

37. Syed O, Walters NJ, Day RM, Kim HW, Knowles JC. Evaluation of decellularization protocols for production of tubular small intestine submucosa scaffolds for use in oesophageal tissue engineering. *Acta Biomater* 2014;**10**:5043–54

38. Baryeh K, Asopa V, Field R, Sochart DH. The outcomes of total hip arthroplasty in rapidly progressive osteoarthritis: a systematic review. *Eur J Orthop Surg Traumatol*. Epub ahead of print 23 September 2022. DOI: 10.1007/s00590-022-03396-8

39. Wang Y, Bao J, Wu Q, Zhou Y, Li Y, Wu X, Shi Y, Li L, Bu H. Method for perfusion decellularization of porcine whole liver and kidney for use as a scaffold for clinical-scale bioengineering engrafts. *Xenotransplantation* 2015;**22**:48–61

40. White LJ, Taylor AJ, Faulk DM, Keane TJ, Saldin LT, Reing JE, Swinehart IT, Turner NJ, Ratner BD, Badylak SF. The impact of detergents on the tissue decellularization process: a ToF-SIMS study. *Acta Biomaterialia* 2017;**50**:207–19